Chandrakesh Shukla[1],

Sunil Kumar Pandey[2]

A Multifunctional VSC for Grid Synchronized SPV System with Mode Transfer Capability

Journal of Electrical Systems

Abstract: **-** This work presents a multifunctional VSC (Voltage Source Converter) for a two-stage single-phase distribution network synchronized battery less PV (Photovoltaic) array generating system with seamless mode transfer capability. This system depicts excellent response at load perturbations and ensures electricity to local loads in day time even in absence of the power grid and cloudy days. The hybrid DSC filter algorithm based control prohibits deterioration of the grid power quality at nonlinear loading besides utility network parameter drifts and the grid voltage distortions. The estimated active load current component and in phase grid voltage unit vector are processed together to make the utility network synchronized PV system multitasking. VSC not only injects surplus power extracted through PV panel to the grid in synchronized mode, but it also provides load harmonics and reactive power compensation. VSC maintains instantaneous power equilibrium not only in grid tied mode but in an islanded mode too under dynamic conditions. This also ensures sinusoidal load voltage in an islanded mode. The THDs (Total Harmonics Distortions) in the utility network current and PCC voltage are found below 5% in both the modes and in compliance with constraints of the IEEE-519 and the IEEE-929 PQ standards.

Keywords: Photovoltaic, Voltage Source Converter, Power Quality, Total Harmonic Distortion, Point of Common Coupling.

1. Introduction

The environmental adversity of fossil fuels, their reserve stock, growing population, and industrialization compels the stakeholder to promote renewable energy based generation to enhance energy security [1-2]. The environmental variations such as irregular irradiance, cloudy days, variation in surroundings temperature, and partial shadowing cause variation in maximum power point (MPP) of PV array. These issues are addressed in [3]. The perturb and observe maximum power point technique (P&O MPPT) is utilized in presented work. The PV array extracted power is intermittent, thus it requires energy storage to support the instantaneous power equilibrium between the PV panel and loads power [4]. Control limitations with a battery energy storage (BES) are discussed in [5], and the issues for power and energy management are reported in [6]. The use of BES merely for energy storage is not a wise option, thus a utility grid is utilized for the exchange of energy and power balance equilibrium. The boost converter adjust duty ratio in accordance to local loads power requirement to maintain power balance equilibrium at an islanded mode while irradiance is available. The use of the utility grid as a buffer needs synchronization of the PV generator to the utility network. The criteria for synchronization are reported in [7]. The single stage and double stage structures are the mostly adopted topologies for grid interfaced PV array systems and offer relative merits and demerits. A hybrid sensitivity theory based control is proposed to control a two stage grid connected PV array in [8]. The two stage battery less topology is adopted in this work. Which ensures electricity to local loads in presence of irradiance unlike the conventional battery less topologies. The DC-DC converter control is investigated in [9-10], only voltage control loop is required in feedback linearization based control of the DC-DC converter in [9], and a hybrid current control is presented to minimize the high frequency voltage source converter (VSC) switching loss in grid synchronized PV converters in [11].

The increased penetration of loads, which are nonlinear in nature like LED lamps, televisions, personal computers, and electronic ballast, cause serious power quality (PQ) concern, particularly harmonics in low voltage power grid [12-15]. The connected nonlinear loads at the PCC (Point of Common Coupling) in a weak power grid distort the PCC voltage [14], thus, worsen the distribution network PQ. Passive filters and centralized active filters are traditionally utilized to enhance the PQ of the grid [15]. The active band-pass filter to mitigate the resonance caused due to grid impedance variation is explored in [16], and the proportional gain of PI (Proportional Integral) controller is adjusted to mitigate the effect of the grid impedance changes. VSC control, which utilizes the active load current amplitude and in phase distribution network voltage unit vector, mitigates the power quality issues apart from powering the loads and injects active power to the power grid. The control techniques to extract the active load current component are investigated in [17-22]. The poor dynamic response of power based phase locked loop (PPLL) [17] caused by the existence of LPF (Low Pass Filter) to

[1] Electrical and Electronics Engineering Department, Maharaja Agrasen Institute of Technology, Delhi-86, Emails: chandrakeshshukla122@gmail.com

mitigate the double frequency component is overcome in enhanced phase lock loop (EPLL). EPLL is subjected to ripples due to the existence of lower order harmonics [18]. SOGI (Second Order Generalized) PLL is prone to DC offset [19], an integrator is added to mitigate the DC offset in SOGI [20]. VSC remains idle at the outage of the grid as reported in [21-22]. A grid interfaced battery energy storage PV system is investigated which functions in an islanded mode at the outage of the public grid in [23]. This system requires battery to operate in standalone mode, thus, it has all the control limitations of PV systems with battery energy storage, and drawbacks pertaining to batteries. The PV configuration investigated in presented work has the capability to function in an islanded mode with no battery energy storage at the outage of the grid, and resynchronized at the storage of the public grid. Moreover, the control algorithm utilized in this work extracts the fundamental frequency sinusoidal reference current, and mitigates the drawbacks of the traditional control algorithms mentioned previously, enhances the utility of VSC and ensures electricity to local loads in day hours.Performance evaluation of this system is demonstrated through simulated response at grid parameters drift and load perturbations. The total harmonic distortions (THDs) in the distribution network current and load voltage are observed below 5%. Salient features of presented work are listed here as follows.

- Unlike conventional control, the control used in present work, ensures grid current power quality concern whilst nonlinear load is integrated at PCC, distorted power network voltage and electrical grid parameter drift conditions. Additionally, mitigates the error in phase and magnitude estimation and pulsating oscillations of extracted output at load current perturbations.
- The compensation capability of VSC is independent of solar irradiance variation, load perturbation, and utility network voltage variation, thus, the grid PQ is enhanced.
- This system has a vigorous response for dynamic solar irradiance, perturbed load, distribution network voltage swell/sag, and at mode transition.
- The enhanced VSC utilization is independent of power output from the PV generator. VSC also feeds reactive fundamental frequency load current component together with load harmonics current components, leading to a reduced VSC payback period.
- This grid tied PV array generator works at low PV panel power conditions efficiently though at reduced power generation.
- This PV array system is derated and feeds loads at outage of the grid, thus ensures supply to loads at the availability of solar irradiance.

2. System Structure

Fig.1 illustrates the utility network synchronized PV panel generator structure. This involves PV panel simulator, DC-DC converter, which adjusts the PV generator voltage according to peak power point in the grid tied mode and as per required load power in an islanded mode, VSC, interfacing inductor, ripple filter, STS (Solid-State Transfer Switch). The STS synchronizes/ desynchronizes the PV array system to a single phase utility grid. The ripple filter mitigates VSC switching ripples and STS switching ripples in PCC voltage and the interfacing inductor mitigates VSC current ripples. This system reduces peak voltage on IGBTs and improves performance under low PV panel power conditions.

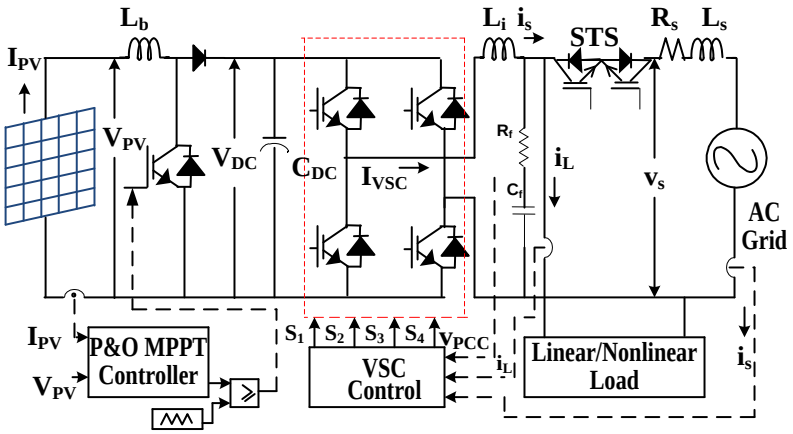

Fig.1 PV array system structure

3. Control Approach

The PV array system control is broadly divided in the power network integrated mode control, standalone mode control, and mode transfer control. The power network integrated mode control approach is depicted in Fig.2-3, and control at an islanded mode is shown in Fig.4.Fig. 2 depict overall control scheme of grid interfaced mode control. Which involves VSC control and DC-DC converter control. The boost converter duty cycle is estimated utilizing P&O MPPT controlto extract peak available power through the PV generator at dynamic irradiance and varying ambient temperature. While at standalone mode, the load instantaneous power requirement is supplied by the PV array generator. This concept is implemented to control the boost converter. The load current peak magnitude (I_{La}), load voltage amplitude (V_A), PV array current (I_{pv}), and the VSC input voltage (V_{DC}) are utilized to evaluate the duty ratio of DC-DC converter in [9-10] as,

$$D_b = 1 - \frac{I_{pv} \times V_{DC}}{I_{La} \times V_A} \tag{1}$$

The hybrid delayed signal cancellation technique is adopted to estimate active load current weight (I_{La}). The active load current weight and the distribution network voltage unit vector (u_x) are utilized to interface the PV panel generator to the utility network. A PV dynamic compensation term (I_{pvc}) lowers the stress on the PI controller and smoothens the boost converter output voltage at dynamic power harnessed through the PV panel and at distribution network voltage sag/swell.

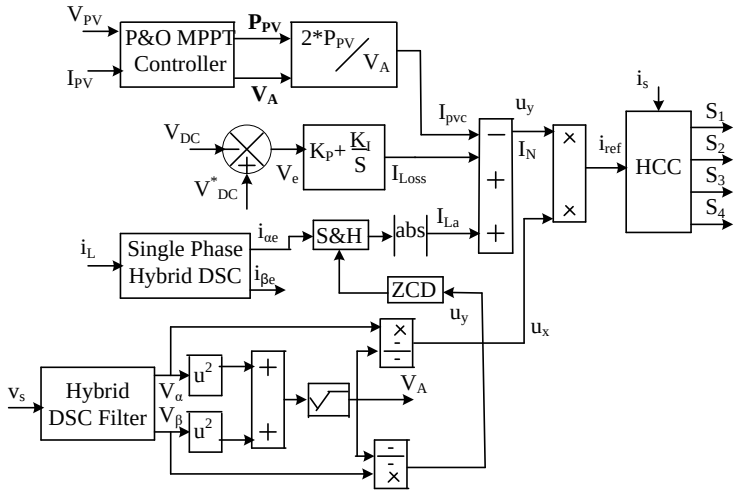

Fig.2 PV system overall control approach

3.1. Grid Tied Mode Control

The distribution network voltage (v_s) is fed to the hybrid delayed signal cancellation (DSC) control algorithm, which mitigates drawbacks of both adaptive and nonadaptive control algorithms and harnesses potentials of both to mitigate harmonics introduced due to VSC switching and grid inductance. Thus, it extracts fundamental frequency utility voltage components ($v_{s\alpha}$) and ($v_{s\beta}$). This fundamental frequency utility voltage orthogonal components ($v_{s\alpha}$, $v_{s\beta}$) are used to extract the network voltage amplitude (V_A) in [15] as,

$$V_A = \sqrt{v_{s\alpha}^2 + v_{s\beta}^2} \tag{2}$$

The utility network synchronizing signal (u_x) and grid voltage quadrature unit template are generated as,

$$u_x = \frac{v_{s\alpha}}{V_A} \tag{3}$$

$$u_y = \frac{v_{s\beta}}{V_A} \tag{4}$$

VSC loss current weight (I_{Loss}), which is drawn from the utility network through the PI controller with proportional gain K_p, and integral gain K_I, during the DC link voltage (V_{DC}) variation to maintain the boost converter output voltage to its reference value (V^*_{DC}) is estimated as,

$$I_{Loss}(l) = I_{Loss}(l-1) + K_p\{(v_e(l) - v_e(l-1)) + K_I(v_e(l)) \quad (5)$$

$$v_e(l) = V_{DC}^{*}(l) - V_{DC}(l) \quad (6)$$

The PV dynamic compensation term (I_{pvc}) is extracted utilizing the PV array generated Power (P_{pv}) and the peak magnitude of PCC voltage (V_A) as,

$$I_{pvc} = \frac{2P_{pv}}{V_A} \quad (7)$$

The active load current weight (I_{La}) is extracted utilizing the hybrid DSC (HDSC) based control, which is shown in Fig.3. This includes adaptive delayed signal cancellation technique and pairs of nonadaptive delayed signal cancellation techniques in cascade.

The double frequency component, phase error, and scaling error appear in the estimated output because the extracted sinusoidal orthogonal components of load current ($i_{\alpha e}$,$i_{\beta e}$) lose orthogonality when the distribution network frequency deviates ($\Delta\omega$') from the nominal grid frequency (ω_n). A compensator overcomes all these issues in the presented work. The control equations to evaluate the distribution network frequency (ω) is in [21] as,

$$I_{de} = i_{\alpha e} \times \cos(\theta) + i_{\alpha e} \times \sin(\theta) \quad (8)$$

$$I_{qe} = i_{\beta e} \times \cos(\theta) - i_{\beta e} \times \sin(\theta) \quad (9)$$

$$\Delta\omega' = \arctan\left(\frac{I_{qe}}{I_{de}}\right) \quad (10)$$

$$\Delta\omega = \Delta\omega'(l-1) + K_{i1}\Delta\omega'_e(l) \quad (11)$$

$$\omega' = \omega_n + \Delta\omega \quad (12)$$

$$\theta = \int \omega' + K_{p1}(\Delta\omega'(l) - \Delta\omega'(l-1)) \quad (13)$$

Where I_{de}, I_{qe} and θ are estimated d-axis and q-axes load currents and extracted reference angle, respectively. The adaptive DSC filter and nonadaptive DSC filter are cascaded to generate the active load current components. The outputs of DSC operator ($i_{L\alpha a}$, $i_{L\beta a}$) are estimated as in [21],

$$i_\beta = i_\alpha \angle -(\pi/2) \quad (14)$$

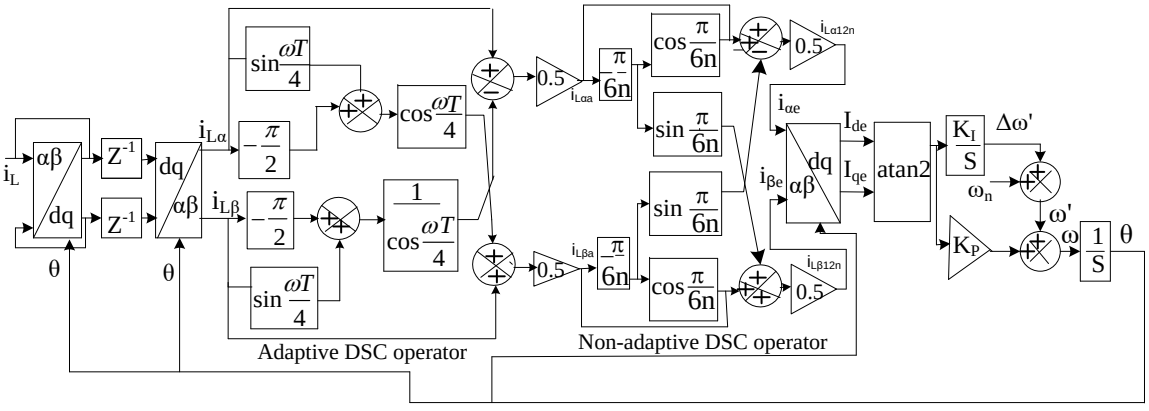

Fig.3 Description of adaptive and non-adaptive DSC approach

$$i_{L\alpha a} = 0.5i_\alpha + j0.5i_\beta \sec(\Delta\omega T/4) + i_\beta \tan(\Delta\omega T/4) \quad (15)$$

$$i_{L\beta a} = 0.5i_\beta - j0.5i_\alpha \sec(\Delta\omega T/4) + i_\alpha \tan(\Delta\omega T/4) \quad (16)$$

The output of first stage, which includes various harmonics load current component beside fundamental frequency sinusoidal load current is utilized by nonadaptive DSC operators to obtain the fundamental frequency

sine and cosine components of load current ($i_{\alpha e}$, $i_{\beta e}$). Governing equations of the nonadaptive DSC operators are given here as in [21],

$$i_{L\alpha 12n} = 0.5i_{L\alpha a} + 0.5i_{L\alpha a}\angle -(\pi/6n)\cos(\pi/6n) - 0.5i_{L\beta a}\angle -(\pi/6n)\sin(\pi/6n) \quad (17)$$

$$i_{L\beta 12n} = 0.5i_{L\beta a} + 0.5i_{L\beta a}\angle -(\pi/6n)\cos(\pi/6n) + 0.5i_{L\alpha a}\angle -(\pi/6n)\sin(\pi/6n) \quad (18)$$

The grid voltage quadrature unit template (u_y) is fed to zero crossing detector to detect positive and negative cosine signal transition. Which is utilized in sample and hold (S&H) circuit to estimate the active load current (I_{La}) as,

$$I_{La} = \mid i_{\alpha e} \mid = I_m \sin(\omega t - \phi)\mid_{\cos(\omega t)=0} = I_m \cos(\phi) \quad (19)$$

The extracted active load current weight (I_{La}), PV array power dynamic current (I_{pvc}), and the PI voltage regulator output as loss current weight are used to evaluate net fundamental frequency distribution network current amplitude as,

$$I_N = I_{La} - I_{pvc} + I_{Loss} \quad (20)$$

The net fundamental frequency power network current amplitude and power network voltage synchronisation vector are processed to obtain reference power network current as,

$$i_{ref} = I_N \times u_x \quad (21)$$

This reference grid current and the observed utility current are compared, and the deviation is injected to HCC (Hysteresis Current Controller). Thus, logic signals for VSC are generated in grid synchronized mode.

3.2. Standalone Mode Control Strategy

This mode control schematic diagram is depicted in Fig.4. The islanded control adjust PCC voltage (v_{pcc}) in proximity to reference voltage (v^*_{pcc}) utilizing a PI controller and bang-bang current controller. The dynamic equation to regulate reference load voltage is given as,

$$v^*_{pcc} = V_p \sin(\omega \times t) \quad (22)$$

The PI controller generates the control current as,

$$i^*_{vsc}(l) = i^*_{vsc}(l-1) + k_{p2}\{v_{e1}(l) - v_{e1}(l-1)\} + k_{i2}v_{e1}(l) \quad (23)$$

The reference VSC current obtained at the output of PI controller and the sensed VSC current are compared, and the difference in VSC current is fed to HCC, thus switching sequences for VSC are obtained.

3.3. Synchronization and Desynchronization Mode Control

A synchronization/desynchronization mode control generates an enable signal for STS switch to integrate and to isolate the PV array generator to/from the distribution grid, thus it ensures smooth transfer of modes, and avoids transients across the load. The selection of grid connected mode or standalone mode is based on the IEEE1547 standard, which is given as in [7],

$$V_{P\min} \le V_s \le V_{P\max};\ f_{P\min} < f_s < f_{P\max};$$
$$\theta_{\min} < \theta_{pcc} < \theta_{\max} \quad (24)$$

The controller generates enabled signal on meeting the criteria, else STS switch received disabled signal (0).

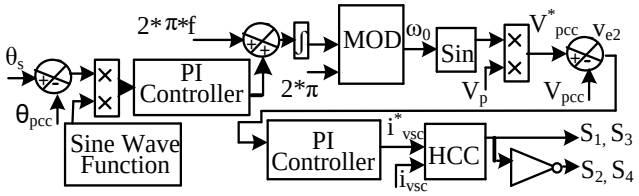

Fig.4 PV array system islanded mode control

4. Results and Discussions

Figs. 5-12 depict the simulated response of the PV system. The HDSC controller response is depicted in Fig.5-6. Whereas the response of the grid synchronised PV-VSC is depicted in Figs.7-12. The response at load perturbation, at distribution static compensator mode (DSTATCOM), and dynamic irradiance is illustrated subsequently in Fig.7, Fig.8, and Fig.9. Fig. 10 demonstrates the system's performance at the grid voltage

variation and mode transition, while FFT analysis of the PV-VSC system at the power network interfaced mode and off-grid mode is depicted in Fig.11 and Fig.12.

3.4. Response of HDSC Control Technique

Figs.5-6 illustrate HDSC control technique response. Figs.5 depicts nonlinear load current (i_L), adaptive DSC operator output currents ($i_{L\alpha a}$, $i_{L\beta a}$), grid frequency sine and cosine load current components ($i_{\alpha e}$, $i_{\beta e}$) which are the output of the nonadaptive DSC operators, VSC loss current (I_{Loss}), net fundamental frequency power grid current amplitude (I_N), the evaluated utility network frequency (ω), and the reference utility current (i_{ref}) at rejection-injection of the load.

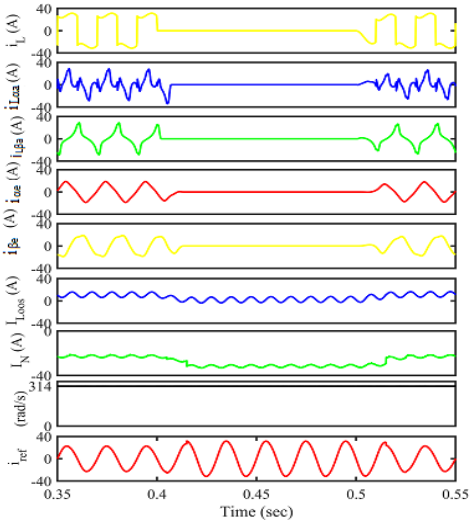

Fig.5 HDSC controller response

The grid current is sinusoidal and increases-decreases on rejection-injection of load. Moreover, the active load current amplitude is following the load current on rejection-injection of the load.

Fig.6 (a) depicts dynamic performance comparison of implemented control algorithm along with moving average filter (MAF) based control algorithm, circular limit cycle oscillator (CLO) based control algorithm and feed forward multiple second order generalized integrator (FMSOGI) based control algorithms to estimate the active component of load current. The proposed control algorithm response at rejection of load reaches to zero at the earliest without oscillations and this controller response attains steady state value accurately in minimum time at injection of load. The settling time of MAF based control algorithm is slightly more than the proposed control algorithm. The CLO based control algorithm has oscillations and thus larger settling time whereas FMSOGI based control algorithm has the largest settling time among all.

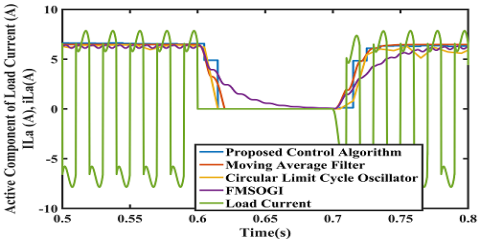

(a)

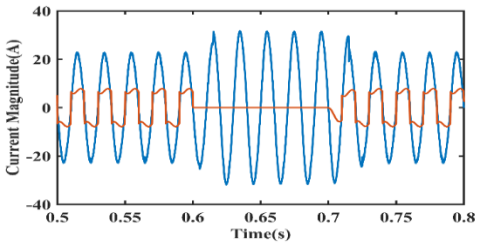

(b)

Fig.6 Response (a) comparison of extracted fundamental frequency load current amplitude at load perturbation (b) phase frequency shift of active load current weight

The proposed control steady state and transient performances are excellent among all investigated control algorithms in the estimated output at load perturbation.

Fig.6 (b) depicts the phase frequency shift of estimated active load current weight. The load current phase and frequency are compared to the power grid current phase and frequency at varying load. Three is no phase frequency shift of controller response at Load perturbation.

3.5. *Performance* at Load perturbation

Figs. 7 depicts load current (i_L), VSC current (i_{vsc}), PV compensation current (I_{pvc}), and the utility current (i_s) at removal-injection of the load. The PV compensation component is unaffected at load perturbations means PV array power generation remains same whereas utility current increases and reduces at rejection and injection of load. Moreover, the VSC current is sinusoidal at rejected load while nonsinusoidal at injected load. This indicates that VSC feeds harmonic current component to load.

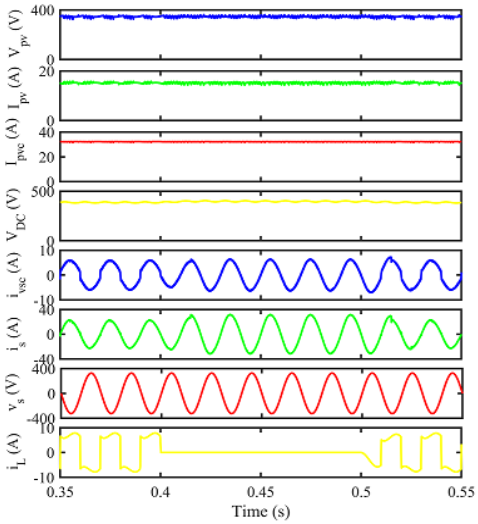

Fig 7. Multifunctional PV-VSC response at load perturbation.

3.6. Response at Distribution Static Compensator Mode

The responses of a SPV generator from PV array generator mode to distribution static compensator (DSTATCOM) mode and from DSTATCOM mode to PV array generator mode are depicted in Fig.8. The PV array current (I_{pv}), load current (i_L), VSC current (i_{vsc}), power network current (i_s), and the grid voltge (V_s) are illustrated. The solar irradiance is varied from 1000W/m^2 to zero and vice-versa. When irradiance is 1000 W/m^2, the power network voltage and current are of opposite phase whereas at zero irradiance both are in the same phase. This concludes that power is injected to the grid during extraction of power through PV panel, while the grid feeds load in DSTATCOM mode. Moreover, the utility current is sinusoidal in PV array generator mode and DSTATCOM mode. Thus, VSC not merely injects active power to loads and to the grid, but the reactive fundamental frequency load current component and load harmonics components at PV array generator mode. Whereas at zero irradiance, VSC is only feeding the reactive fundamental frequency load current component and load harmonics current components. This evident the harmonic compensation capability of VSC.

3.7. Response at Varying Irradiance

The PV-VSC system dynamic performance in response to changing irradiance is depicted in Fig. 9. The PV panel current (I_{pv}), VSC current (i_{vsc}), load current (i_L), and utility network current (i_s) are illustrated. The irradiance is changed from 1000W/m^2 to 500W/m^2, and vice-versa. The power fed into the power network increases and reduces when the irradiance is increased and decreased, respectively. The boost converter output voltage (V_{DC}) is steady at increased or decreased irradiance since the boost converter duty cycle (D) changes to adjust the peak power point at the variation in irradiance.

3.8. Response at Grid voltage Variation

The PV-VSC performance at the distribution grid voltage variationis depicted in Fig.10. Fig. 10(a) shows behaviour of PV-VSC at the distribution network voltage deviation. The grid voltage is drifted from 230V to 248V at t=0.7s, while the utility network voltage is varied from 248V to 212V at t=0.8s. The VSC input voltage (V_{DC}), the PV panel voltage (V_{pv}), and the PV panel current (I_{pv}) remain unchanged meaning that steady power output through the PV panel. The load current, the extracted load current amplitude and the utility current vary

according to the utility grid voltage. There is an increase and decrease in the load current when the voltage sag and the voltage swell in the utility voltage occur. Consequently, there is a reduction and an increment in the grid current too.

The SPV generator response is shown in Fig.10 (b) at the grid voltage outage and restoration. The power network voltage outage takes place at t=0.7s, STS switch is opened and an islanded mode control adjusts the load voltage to its reference value. The power injected to the grid is decreased to zero, whereas the SPV generator power output is decreased according to load requirement to balance the power equilibrium. Moreover, the transient free PCC voltage and transient free load current guarantee smooth mode transfer among the power network interfaced mode to off grid mode, and conversely on restoration of healthy grid condition at t=0.8s.

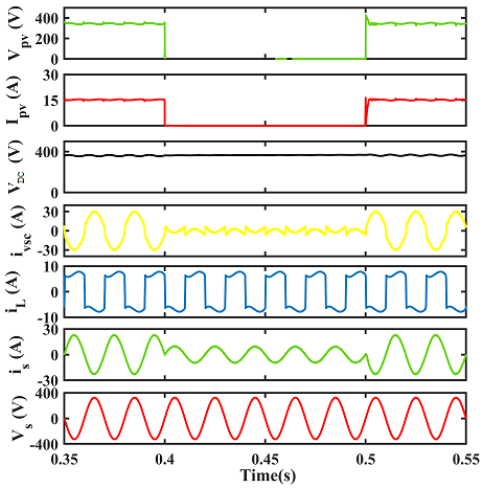

Fig.8 Response at distribution static compensator mode

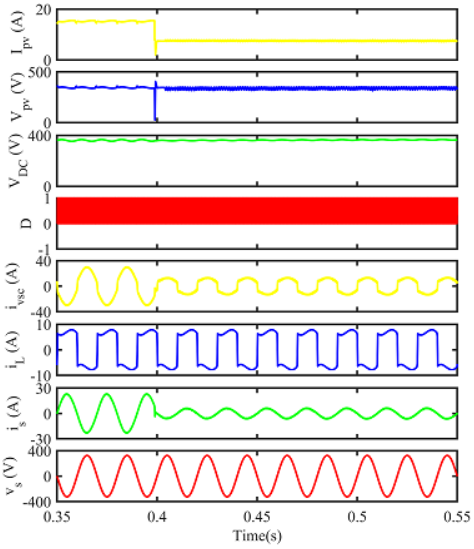

Fig.9 Response at dynamic irradiance

3.9. PV-VSC Harmonic Performance

The harmonic performance of the power grid parameters at distorted load current is depicted in Figs. 11(a)-(c) in the power grid synchronized mode.

The grid voltage, utility network current, and load current fast Fourier transform analysis are depicted subsequently in Fig 11(a), Fig.11 (b), and Fig.11(c).

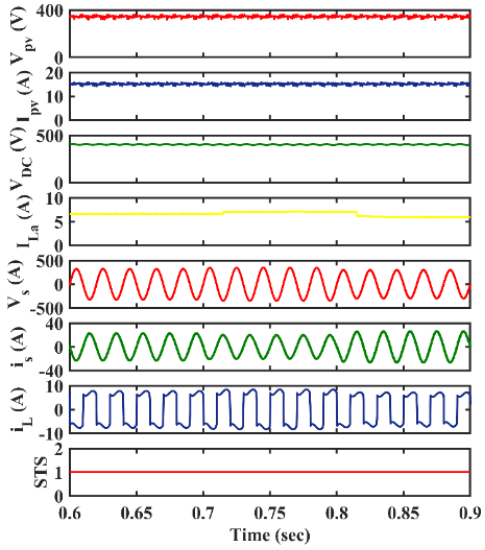

(a)

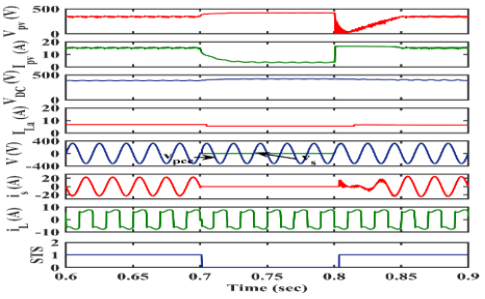

(b)

Fig.10.PV-VSC response at (a) grid voltage variations. (b) transition mode.

The PCC voltage FFT analysis and load current FFT analysis are illustrated in Fig. 12(a) and Fig.12 (b), respectively. The load voltage THD is 0.94% and load current THD is 42.17%. The load current harmonic distortion is mitigated to 1.82% in the distribution network current. Whereas the load voltage harmonic distortions and load current THD are 2.93%, and 4.47 %, respectively. Thus, the PQ (Power Quality) enhancement feature of the grid synchronized PV array generator is evident.

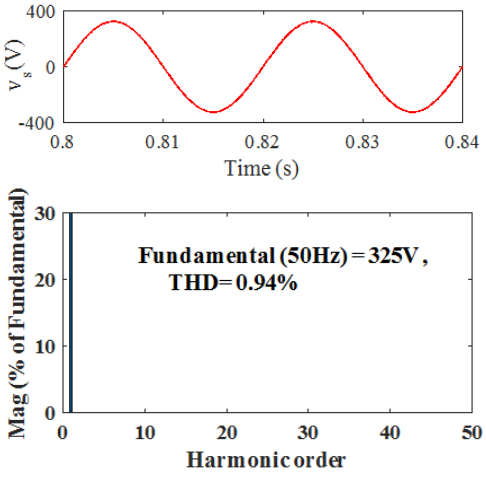

(a)

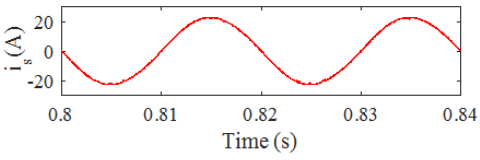

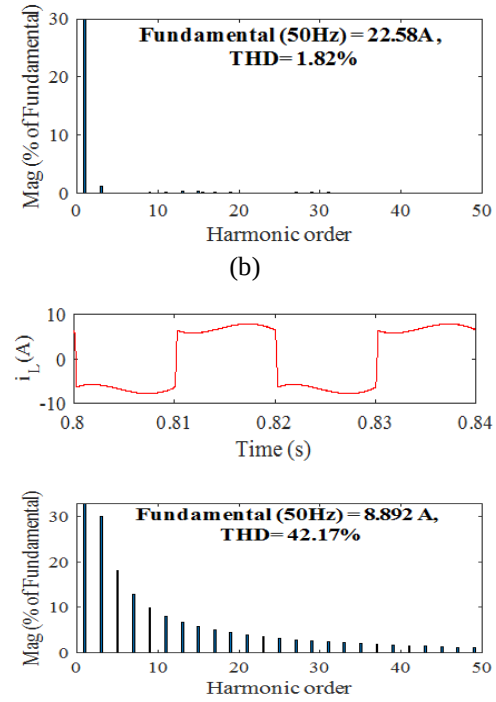

Fig.11 FFT Analyses at grid interfaced mode (a) utility voltage, (b) distribution grid current, (c)load current

.

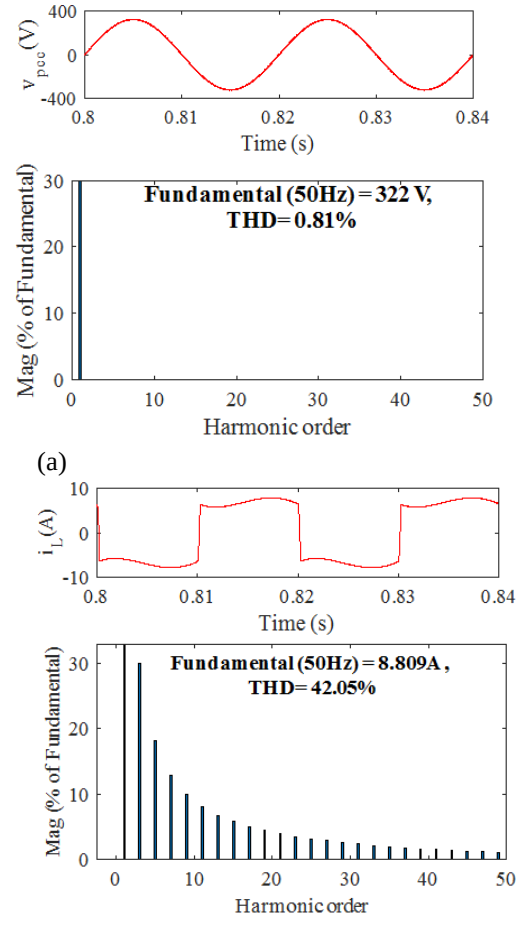

Fig.12 FFT analyses at islanded mode (a) PCC voltage, (b) load current network

5. Conclusion

The multifunctional feature of VSC of the grid integrated battery less SPV system is investigated in MATLAB Simulink environment. The implemented PV array topology secures electricity to the local loads in day time at the outage and restoration of the utility grid seamlessly. The performance similar to battery integrated topologies is obtained in presence of irradiance at an islanded mode as well as in the grid tied mode. THD of the PCC voltage and the utility grid current in both the grid interfaced mode and an islanded mode in accordance to IEEE-519 standard implicit that the grid current power quality is ensured in the presence of nonlinear load connected at PCC and the grid parameter deviations. The transient response of this system at the power network parameters changes like voltage swell, voltage sag, dynamic irradiance, and under load perturbations, is investigated in detail. This system has excellent performance both at transient conditions and steady state conditions.

Appendices

Simulation Data:PV rating, P_{mpp}=5kW, voltage (V_{oc})= 32.9VV, I_{sc}=8.21A, N_{se}=54, N_s=13, N_p=2, L_b=5mH, C_{DC}=3100µF,L_i=2.5mH, Ripple filter R_f=5Ω, C_f=7.5µF, single phase power grid 230V, 50Hz, RL load followed by diode bridge: 30Ω, 200mH, PI controller gains, K_p=0.2, K_I=0.01, Frequency compensator gains K_{p1}=0.01, K_{I1}=0.001, T_s=5microsecond.Islanded mode PI controller gains K_{p2}=5, K_{I2}=-20.

References

[1] M. S. Uney and N. Cetinkaya. “Comparison of CO2 emissions fossil fuel based energy generation plants and plants with Renewable Energy sources,” *International Conference on Electronics, Computer and Artificial Intelligence (ECAI)*, Bucharest, pp. 29-34, 2014.

[2] Nuno Bento, MattiaBorello, and Gianfranco Gianfrate, “Market Pull Policies to Promote Renewable Energies: A QuantativeAssesement of Tendering Implementation,” *Journal of Cleaner Production*, vol. 248, March 2020.

[3] I. Pervez, A. Pervez, M. Tariq, A. Sarwar, R.K. Chakrabortty and M.J. Ryan, “Rapid and Robust Adaptive Jaya (Ajaya) Based Maximum Power Point Tracking of a PV-Based Generation System,”*IEEE Access*, vol.9, pp.48679-48703, 2021.

[4] A.A. Abdalla, M.S.E. Moursi, T.H.M. El-Fouly and K.H.A. Hosani, “Reliant Monotonic Charging Controllers for Parallel-Connected Battery Storage Units to Reduce PV Power Ramp Rate and Battery Aging,” *IEEE Transactions on Smart Grid*, vol. 14, no.6, pp.4424-4438, Nov. 2023.

[5] S. Duryea, S. Islam, and W. Lawrance, “A battery management system for stand-alone photovoltaic energy systems,” *IEEE Industry Applications Magazine*, vol.7, no.3, pp.67- 72, Jun 2001.

[6] S. Dutta, D. Debnath and K. Chatterjee, “A Grid-Connected Single-Phase Transformer less Inverter Controlling Two Solar PV Arrays Operating Under Different Atmospheric Conditions,” *IEEE Transactions on Industrial Electronics*, vol. 65, no. 1, pp. 374-385, Jan. 2018.

[7] IEEE Standard for Interconnection and Interoperability of Distributed Energy Resources with Associated Electric Power Systems Interfaces-Amendment 1: To Provide More Flexibility for Adoption of Abnormal Operating Performance Category III, “*IEEE Std 1547a-2020* (*Amendment to IEEE Std 1547-2018*),” pp.1-16, April 2020.

[8] X. Fu, Q. Fu, and W. Tang, “Grid Connected Technique based on µ Theory for a Two Stage PV Structure,” *IET Power Electronics*, vol. 12, issue 6, pp. 1545-1553, May 2019.

[9] R. Errouissi, A. Al-Durra, S. M. Muyeen, and A. El Aroudi, “ Robust Feed Back Linearization Control of a Boost Converter Feeding a Grid Tied Inverter for PV applications,” *IET Power Electronics*, vol. 11, issue 3, pp.557-565, March 2018.

[10] N. Mohan, T. M. Undeland, and W. P. Robbins, Power electronics: converters, applications and design, 3rd ed. New Delhi, India: John Wiley & sons Inc., 2014.

[11] J. Lin, S. Cheng, and A. Shen,” Carrier Overlapping PWM Based Hybrid Current Control Strategy Applied to Two Stage Grid Connected PV inverters*,” IET Power Electronics*, vol. 11, issue 1, pp. 182-191, Jan. 2018.

[12] A. Mansoor, W.M. Gradv, P.T. Staats, R.S. Thallam, M.T. Dovle, and M.J. Samotvi, “ Predicting the Net Harmonics Currents Produced by Large Numbers of Distributed Single Phase Computers loads,” *IEEE Trans. Power Delivery*, vol.10, no.4, PP 2001-2006, Oct 1994.

[13] G. Lou, S.Li, W. Gu and Q. Yang, “Distributed Harmonic Power Sharing with Voltage Distortion Suppression in Islanded Microgrids Considering Non-linear Loads,” *CSEE Journal of Power and Energy Systems*, vol.10, no.1, pp. 117-128, jan. 2024.

[14] D. J. Pileggi, E. M. Gulachenski, C. E. Root, T. J. Gentile and A. E. Emanuel, “The effect of modern compact fluorescent lights on voltage distortion,” *IEEE Trans. Power Delivery*, vol.8, no.3, Hosanipp.1451-1459, July 1993.

[15] B. Singh, A. Chandra, and K. Haddad, Power Quality: Problems and Mitigation Techniques. New Delhi, India: Wiley, Jan. 2017.

[16] H. Goh, M. Armstrong, B. Zahawi, “Adaptive Control Technique for Suppression of Resonance in Grid-Connected PV Inverters,” *IET Power Electronics*, vol.12, issue 6, pp.1479-1486, May 2019.

[17] J. Xu, H. Qian, S. Bian, Y. Hu and S. Xie, "Comparative Study of Single-Phase Phase-Locked Loops for Grid-Connected Inverters under Non-Ideal Grid Conditions, "*CSEE Journal of Power Energy Systems*, vol.8, no.1, pp.155-164, Jan. 2022.

[18] S. Luo and F. Wu, "Improved Two-Phase Stationary Frame EPLL to Eliminate the Effect of Input Harmonics, Unbalance and DC offsets, *"IEEE Transactions on Industrial Informatics*, vol.13, no. 6, pp. 2855-2863, Dec. 2017.

[19] J. Yu, W. Shi, J. Li, L.Deng and M. Pei, "A Discrete-Time Non-Adaptive SOGI-Based Frequency-Locked Loop," *IEEE Transactions on Power Systems*, vol.35, no.6,pp.4912-4915, Nov.2020.

[20] M. Xie, H. Wen, C. Zhu and Y. Yang, "DC Offset Rejection Improvement in Single-Phase SOGI-PLL Algorithms: Methods Review and Experimental Evaluation," *IEEE Access*, vol.5, pp.12810-12819, 2017.

[21] S. K. Pandey and B. Singh, "Hybrid DSC with Compensation Capability Based Control for Grid Integrated SPV System," *IEEE Power India Inter, Conf. (PIICON),*Sonepat, India, pp. 1-6, 2020.

[22] Sunaina. Singh, SeemaKewat, Bhim Singh, and Bijaya K. Panigrahi, "Enhanced Momentum LMS based Control Technique for Grid Tied Solar System," *IET Power Electronics*, vol.13, no. 13, pp. 2767-2774, October 2020.

[23] M. Kashif and B. Singh, "Extended FOGI-FLL Based Seamless Control of Grid Synchronized BES-PV Fed Water Pump System, "*IEEE Transactions on Power Electronics*, vol.39, no.1, pp. 1624-1635, Jan. 2024.